Published in final edited form as:
J Nat Prod. 2013 September 27; 76(9): . doi:10.1021/np400308w.

Herbimycins D-F, Ansamycin Analogues from *Streptomyces* sp. RM-7-15

Khaled A. Shaaban[†], **Xiachang Wang**[†], **Sherif I. Elshahawi**[†], **Larissa V. Ponomareva**[†], **Manjula Sunkara**[‡], **Gregory C. Copley**[§], **James C. Hower**[§], **Andrew J. Morris**[‡], **Madan K. Kharel**[*,†], and **Jon S. Thorson**[*,†]

[†]Center for Pharmaceutical Research and Innovation, College of Pharmacy, University of Kentucky, 789 South Limestone Street, Lexington, Kentucky 40536-0596, United States

[‡]Division of Cardiovascular Medicine, University of Kentucky, Lexington, KY 40536, United States

[§]Center for Applied Energy Research, University of Kentucky, Lexington, KY, 40511, United States

Abstract

Bacterial strains belonging to the class actinomycetes were isolated from the soil near a thermal vent of the Ruth Mullins coal fire (Appalachian mountains of Eastern Kentucky). High resolution electrospray ionization mass spectrometry (HR-ESI-MS) and ultraviolet (UV) absorption profiles of metabolites from one of the isolates (*Streptomyces* sp. RM-7-15) revealed the presence of a unique set of metabolites ultimately determined to be herbimycins D-F (**1**–**3**). In addition, herbimycin A (**4**), dihydroherbimycin A (TAN 420E) (**7**), and the structurally distinct antibiotic bicycylomycin were isolated from the crude extract of *Streptomyces* sp. RM-7-15. Herbimycins A, D-F (**1**–**3**) displayed comparable binding affinities to the Hsp90α. While the new analogues were found to be inactive in cancer cell cytotoxicity and antimicrobial assays, they may offer new insights in the context of non-toxic ansamycin-based Hsp90 inhibitors for the treatment of neurodegenerative disease.

INTRODUCTION

Ansamycins, a clinically important class of molecules produced predominantly by actinobacteria species, are characterized by the presence of a mC7N core which originates from 3-amino-5-hydroxybenzoate (AHBA).[1–5] Multimodular polyketide synthases (PKSs) subsequently catalyze a sequential addition of acetate and propionate at the carboxylic acid group of AHBA prior to the formation of macrolactam ring.[6] The folding and cyclization of the newly formed polyketide chain ultimately contribute to the formation of two main subclasses of ansamycins - the benzoquinone and napthoquinone macrolactams. Napthoquinone ansamycins are best known for their antimicrobial activities mediated via a specific inhibition of bacterial RNA polymerase,[7] whereas the benzoquinone ansamycins have been identified as inhibitors of eukaryotic Hsp90, an important cancer target.[8] Members of each subclass have advanced to clinical use with several napthoquinone analogues (such as rifampin, rifabutin, and rifapentine) used for the treatment of leprosy, tuberculosis, and AIDS-related mycobacterial infections,[9–13] and analogues of the potent benzoquinone-based Hsp90 inhibitors (such as tanespimycin and alvespimycin)[14–17]

[*]To whom correspondence should be addressed: jsthorson@uky.edu; Madan.Kharel@uky.edu.

Supporting Information Available: UV, HPLC-MS, NMR (1D and 2D), and HR-ESI-MS spectra of herbimycins D-F (**1**–**3**), in addition to the spectroscopic data of bicyclomycin. This material is available free of charge via the Internet at http://pubs.acs.org.

advancing to late stage clinical development.[18,19] The diverse array of biological activities displayed by ansamycins (including antitumor, antibacterial, antiviral, antifungal, antiprotozoal, and immunosuppressive), continue to stimulate efforts to discover and/or synthesize novel ansamycins.[20–23]

As a part of our ongoing natural product discovery initiative, we are investigating soil actinomycetes collected near thermal vents emanating from a range of underground coal mine fire sites throughout Appalachia.[24–27] AntiBase [28] comparison of HPLC-high resolution mass spectrometry (HPLC-HR-MS) profiles of the culture extracts of 23 actinomycete strains isolated from a single soil sample collected near a thermal vent associated with the Ruth Mullins underground coal mine fire indicated that one of the isolates, namely *Streptomyces* sp. RM-7-15, was capable of unique metabolite production. In this report, we describe the fermentation of *Streptomyces* sp. RM-7-15, and the isolation and structure elucidation of three new ansamycin analogues, herbimycins D-F (**1**–**3**), along with the known metabolites herbimycin A (**4**), dihydroherbimycin A (**7**) and the structurally distinct antibiotic bicyclomycin. Herbimycin E (**2**) represents the first example of an ansamycin which harbors a unique *ortho*-quinone moiety.

RESULTS AND DISCUSSION

Preliminary HPLC/MS analysis of the extract generated from a 50 mL fermentation of *Streptomyces* sp. RM-7-15 revealed three predominant metabolites which lacked an obvious UV signature or MS match in the AntiBase 2012 database, suggesting the potential of *Streptomyces* sp. RM-7-15 to produce new metabolites. To generate sufficient material for characterization (chemical and biological), the fermentation was scaled to 8 L and separate extraction of the culture broth and mycelial cake afforded 14.32 g and 65.4 g of crude material, respectively (see materials and methods). LC-MS revealed the targeted metabolites within the culture broth fraction and TLC analysis of the extract of the culture broth exhibited a yellow spot along with several UV-active spots (254 nm), which turned blue-green by staining with anisaldehyde/sulfuric acid spraying reagent. Normal phase silica gel flash fractionation of the crude extract followed by HPLC purification of selected fractions led to the isolation of three new ansamycin analogues, herbimycins D (**1**, 4.3 mg/L), E (**2**; 2.1 mg/L) and F (**3**; 0.28 mg/L) (Supporting Information, Figure S2). In the course of the work up process, three additional known compounds - herbimycin A (**4**), dihydro-herbimycin A (**7**; TAN 420E), and the peptide antibiotic bicyclomycin (Supporting Information, Figures S25–S32) - were also isolated and characterized.

Compound **1** was isolated as a pale yellow solid material which displayed maximum UV absorbance at 246 nm. Compound **1** display a R_f of 0.44 via TLC (15% MeOH-CH_2Cl_2) and in the presence of the anisaldehyde/sulfuric acid indicator the color of compound **1** on the TLC plate changed over time from pale yellow→ dark-blue→yellowish-green→reddish-brown. The molecular formula of **1** was deduced as $C_{32}H_{45}N_3O_9S$ (*m/z* 648.2946 $[M + H]^+$) on the basis of HR-ESI-MS and of ^1H and ^{13}C NMR data. The proton NMR spectrum of **1** in CD_3OD (Table 1) displayed one singlet aromatic signal at δ 6.73, four olefinic proton signals at δ 6.37 (t, *J* = 11.6 Hz), 6.02 (brm), 5.20 (d, *J* = 10.4 Hz) and 5.12 (brm), along with an oxygenated methine signal at δ 4.69 (brm). Four oxygenated methine signals along with four methoxy signals were observed in the range of δ 3.87~3.00 ppm. Additionally, the ^1H NMR spectrum displayed two methine signals at δ 2.38 (m) and 2.26 (m), one methylene group at δ 1.74–1.60, along with four methyl signals at δ 2.01 (s), 1.23 (brs), 0.98 (d, *J* = 6.4 Hz) and 0.69 (brd, *J* = 5.3 Hz). These data implied the structure of **1** to be closely related to herbimycin A (**3**) and potentially share an identical macrolactam ring. While one of the two aromatic singlet protons observed in ^1H NMR of herbimycin A (**3**) was missing

in **1**, the presence of two geminally coupled proton signals observed at 3.62 (1H, d, J = 14.8) and 3.31 (1H, d, J = 14.8) were indicative of the presence of a CH_2 group in a ring.

The ^{13}C NMR/HSQC spectra (Table 1) of compound **1** indicated the presence of 32 carbon atoms and also revealed its close structural similarity to herbimycin A, and its derivative TAN420D. The two carbonyl signals observed for herbimycin A were missing in **1**, and instead, two quaternary carbons were detected at δ 148.1 (C_q-21) and 126.9 (C_q-18). Two additional carbon signals observed in ^{13}C NMR spectrum of compound **1** at δ 166.8 and 30.0 (CH_2) suggested the presence of a quaternary (C_q) and a methylene (CH_2) carbon, respectively. The upfield chemical shift of the methylene group (δ_C 30.0) also indicated its attachment to a sulfur atom. All the remaining chemical shifts of the carbon signals of **1** were very similar to those observed in herbimycin A and TAN 420E, implicating a herbimycin A analogue bearing an additional C_2H_3NS structural unit at C_q-19 of the benzene ring. ^1H–^1H COSY and HMBC correlations (Figure 2) of compound **1** confirmed this structural hypothesis via observed $^3J/^2J$ correlations from methylene protons (CH_2-26) to C_q-19 (δ_C 117.6) and C_q-27 (δ_C 166.8). The relatively weaker signal observed at 166.8 ppm for C_q-27 suggested an amide carbonyl carbon and additional observed HMBC correlations between the aromatic proton H-17 and C_q-19 (δ_C 117.6), C_q-21 (δ_C 148.1) and CH-15 (δ_C 82.7) confirmed the attachment of a mercaptoacetamide moiety at C-19 position. This was further confirmed by comparison to the biosynthetically engineered 4,5-dihydro-thiazinogeldanamycin which features an identical mercaptoacetamide substitution pattern.[29] Remaining ^1H–^1H COSY and HMBC correlations (Figure 2) confirmed structure **1** as 4,5-dihydro-thiazinoherbimycin A. The stereocenters of compound **1** were indirectly established on the basis of coupling constants, NOESY correlations (Figure 2) and on the basis of close NMR similarities to that of **1** and herbimycin A. NOESY cross peaks observed between 15-OCH_3 and H-14, CH_3-25 and H-15, 12-OCH_3 and H-14, and CH_3-24 and 11-OCH_3 established the relative configurations at the stereocenters 10, 11, 12, 14 and15 positions as depicted in Figure 2. A comparison of chemical shifts and coupling constants with the reported analogues provided the basis for the proposed relative configuration at the C-6 position as depicted in Figure 2. Additional NOESY correlations observed between CH_3-22 and H-4, H-4 and H-5, CH_3-23 and H-6, and H-7 and H-10 established the conformation of the double bonds. The strong NOE cross peak observed between CH_3-24 and 7-H established the relative configuration at the C-7 position (Supporting Information, Figure S13). Thus, comparative analyses of spectral data of **1** and the data of related molecules reported in the literature further confirmed the structure of **1**. While a few mercaptoacetamide-bearing ansamycins have been reported,[30–32] to the best of our knowledge this is the first reported example within the context of the herbimycins (Figure 1). As compound **1** represents a new herbimycin analogue, it has been named herbimycin D.

Compound **2** was isolated as a purple solid. On TLC, compound **2** was visible under UV (λ = 254 nm) and converted to a dark-blue color in the presence of anisaldehyde-sulfuric acid. The UV spectrum of compound **2** displayed three absorption maxima at 232, 246 and 532 nm, indicative of the presence of a quinone. Based on HR-ESI-MS data (*m/z* 591.2917 $[M + H]^+$, calcd for $C_{30}H_{43}N_2O_{10}$, 591.2912) the molecular formula of **2** was deduced as $C_{30}H_{42}N_2O_{10}$. The 16 *amu* difference between **2** and herbimycin A suggested the presence of an extra oxygen atom and a comparison of ^1H NMR, ^{13}C NMR and HSQC spectra in CD_3OD (Table 1) indicated compound **1**, **2** and herbimycin A to share a common macrolactam ring system. Key differences were observed in the aromatic ring where **2** displayed an additional oxygenated quaternary carbon. This gave rise to two possible oxygen substitutions –at C-17 (fragment A, Figure 3) or at C-19 position (Fragment B, Figure 3). While there exists prior precedence of 17-OCH_3-substituted geldanamycins, the cross peak observed between H-17 (δ_H 6.24) and 15-OCH_3 (δ_H 3.32) in the NOESY spectrum of **2** supported the alternative C-19 substitution pattern where the molecule could

undergo keto-enol tautomerization to yield the third fragment **C**. A significant difference in the ^{13}C NMR shifts of C-18, C-19 and C-21 carbon signals (δ_C 190.1, 181.7 and 163.8) of **2** and those found in the benzoquinone moiety of herbimycin A (**3**, δ_C 188.1 and 184.3) indicated that compound **2** contains an *ortho*-quinone moiety as indicated in fragment **C**. This also provides a plausible explanation for different colors displayed by compounds **2** (purple) and herbimycin A (yellow). NMR chemical shifts observed in **2** were in good agreement with those of the fully characterized *ortho*-quinone natural product 7-hydroxy-8-methoxymalbranicin-5,6-quinone.[33] The remaining HMBC correlations (Figure 3) and NMR data (Table 1) further confirmed **2** as a new analogue of herbimycin A, and this molecule was subsequently named as herbimycin E (**2**) (Figure 4).

Compound **3** was obtained as white solid from the mycelium sub-fraction FIV after a sequence of chromatographic separations. Compound **3** on TLC (R_f of 0.21, 15% MeOH-CH_2Cl_2) did not absorb UV light, but gave a reddish-brown color with anisaldehyde-sulfuric acid. The molecular weight of **3** was confirmed as *m/z* 548 Dalton by APCI and ESI MS. (+)-HRESI MS confirmed the molecular formula of **3** as $C_{28}H_{40}N_2O_9$ (*m/z* 571.2629 [M + Na]$^+$, calcd for $C_{28}H_{40}N_2O_9Na$, 571.2626), with one less double bond equivalent than **2**.

The proton NMR spectrum of **3** in CD_3OD (Table 1) displayed two *m*-coupled protons at δ 6.24 (*J* = 3.0 Hz) and 6.21 (*J* = 2.5 Hz) in the aromatic region. One doublet proton at δ 5.39 (d, *J* = 10.5) was observed within the olefinic region, consistent with the presence of a C-8/C-9 double bond as previously observed in compounds **1** and **2**. In addition, the four herbimycin analogue signature methyl signals CH_3-22, CH_3-23, CH_3-24 and CH_3-25 were also observed in compound **3** at δ 1.31 (s), 1.52 (s), 1.06 (d, *J* = 6.5) and 0.76 (d, *J* = 6.0) respectively. Distinct from the four methoxy signals of **1** and **2,** only two methoxy signals at δ 3.46 (s) and 3.44 (s) were observed for **3**. The conjugated double bonds found at C-2 and C-4 of **1** were also missing in **3** based upon both NMR and reduced UV light absorption. The ^{13}C NMR/HSQC spectra (Table 1) of compound **3** indicated the presence of 28 carbon atoms and also revealed its close structural similarity to herbimycin D (**1**). The main differences were the presence of sp^3 carbon signals at δ 80.1 (Cq), 50.2 (CH_2) and 49.9 (CH_2), the presence of an extra ketonic carbonyl at δ 205.8 (C=O) group and the absence of the C-19 mercaptoacetamide moiety. ^1H–^1H COSY and HMBC analyses of compound **3** (Figure 5), confirmed **3** to lack the C-11 and C-15 methoxy groups of **1**. Furthermore, the ^3J HMBC correlations observed in **3** from CH_3-22 (δ_C 23.1) to CH_2-3 (δ_C 50.2) and CO-1 (δ_C 177.5) along with the ^2J correlations to C-2 (δ_C 80.1) confirmed the lack of the double bond between C-2 and C-3. The observed ^2J and ^3J HMBC couplings from CH_2-3 to C-4 (δ_C 205.8) and C-1 (δ_C 177.5) respectively, suggested the presence of the ketonic group at C-4. Similar to herbimycins A-C, TAN 420A-C and E, and macbecin I and II, the two *m*-coupled proton signals observed in the ^1H NMR spectrum of **3** were confirmed to derive from C-17 and C-19, consistent with the replacement of the C-19 mercaptoacetamide by a hydroquinone moiety. Of the two possible structures consistent with the spectroscopic data (**3**, Figure 5 and **14**, Figure 6) the notable stability of molecule at the room temperature and the lack of HMBC correlation from H-11 to C-2, served as a basis for elimination of **14**. The small H-11 to C-HMBC coupling observed provides further evidence of the C-11/C-21ether linkage and importantly, a similar linkage was recently reported within the geldanamycin analogue thiazinogeldanamycin.[29] All the remaining HMBC and COSY correlations were in full agreement with structure **3** (Figure 5). The configurations at C-2, 6, 7, 10, 11, 12 and 14 of **3** were predicted on the basis of the NOESY spectra analysis and on the similarity of other NMR data (Figure 5). The α-orientation of the methyl group CH_3-22 was deduced from the lack of the NOESY correlations between CH_3-22 and 6-OCH_3. The remaining NOESY correlations (Figure 5) were in full agreement with structure **3.** The compound **3**

represents an unusual new herbimycin analogue and was subsequently named as herbimycin F.

Less than 25 bacterial *ortho*-quinones metabolites have been reported thus far (AntiBase, 2012) and within this context, herbimycin E (**2**) reported herein represents the first example of an *ortho*-quinone ansamycin. The unusual intramolecular etheric linkage observed in herbimycin F (**3**) further expands the structural diversity of known macrolactam natural products. Unlike geldanamycin and herbimycin A, which were both equipotent in cancer cell line cytotoxicity assays (A549, IC_{50} 0.15 μM), the new analogues (herbimycins D-F) did not exhibit any cytotoxicity (at or below 10 μM), antibacterial and antifungal activities (at 125 μM). These results are consistent with prior studies that illustrated how subtle modifications of the ansamycin quinone could dramatically alter the cytoxicity of corresponding analogues.[34] Surprisingly, the newly identified herbimycins C-F were found to bind the Hsp90α *N*-terminal domain with similar affinity to that of geldanamycin and herbimycin A based upon a FITC-labeled geldanamycin displacement assay previously used to assess affinity for the Hsp90α ATP-site (Figure 7).[35] The identification of 'non-toxic' Hsp90 inhibitors remain of interest in the context of neurodegenerative disease as inhibition of Hsp90 can induce the heat shock response, restore Hsp70 levels and thereby potentially counter various aspects of Alzheimer's disease pathogenesis.[36] Thus, apparent Hsp90α affinity of the less toxic herbimycins D-F may provide a new avenue for the further development of neurodegenerative leads.

Experimental Section

General Experimental Procedures

UV spectra were recorded on an Ultrospec 8000 spectrometer (GE, Pittsburgh, USA). NMR spectra were measured on Varian VnmrJ 400 (^{1}H, 399.8 MHz; ^{13}C, 100.5 MHz) spectrometer and the δ-values were referenced to the respective solvent signals. HR-ESI-MS spectra were recorded on AB SCIEX Triple TOF® 5600 System (AB Sciex, Framingham, MA, USA). HPLC-MS analyses were carried out in Waters 2695 LC module (Waters corp. Milford, MA, USA) using a Symmetry Anal C_{18} 5 μm column (4.6 × 250 mm). Gradient elution conditions - solvent A: H_2O, solvent B: acetonitrile; flow rate: 0.5 mL/min; 0–4 min 90% A and 10% B, 4–22 min, 90–0% A, 22–27 min 0% A and 100% B, 27–29 min 0–90% A, 29–35 min 90% A and 10 % B. For preparative scale separation, a Phenomenex C_{18} column (10 × 250 mm, 5 μm) was used on a Varian ProStar Model 210 equipped with a photodiode diode array detector. Preparative separation conditions - **s**olvent A: H_2O, solvent B: acetonitrile; flow rate: 5.0 mL min^{-1}; 0–2 min 75% A and 25% B, 2–15 min, 75-0% A, 15–17 min 0% A and 100 % B, 17–18 min 0–75% A, 18–19 min 75% A and 25% B. All solvents used were of ACS grade and purchased from the Pharmco-AAPER (Brookfield, CT). Silica gel (230 400 mesh) for column chromatography was purchased from Silicycle (Quebec City, Canada). R_f values were measured on Polygram SIL G/UV_{254} (Macherey-Nagel & Co., Dueren, Germany). Amberlite XAD-16 was obtained from Sigma-Aldrich, St. Louis, MO, USA. Size exclusion chromatography was performed on Sephadex LH-20 (25 ~ 100 μm, GE Healthcare, Little Chalfont, United Kingdom).

Isolation of *Streptomyces* sp. RM-7-15 and preliminary screening of the metabolites

The soil sample was collected from the Ruth Mullins underground mine fire, Perry County, KY (coordinates: N 37° 18.725′ and W 83° 10.3335′). *Streptomyces* sp. RM-7-15 was isolated from soil following minor modifications of a previously reported protocol.[37] Specifically, soil sample (0.5 g) was suspended in 1.0 mL of sterile H_2O and the suspension was heated to 75 °C for 10 minutes to eliminate non-sporulating bacteria. Following serial dilution (10^{-1}, 10^{-2}, 10^{-3}) of the suspension with sterile water, a 100 μL aliquot was spread

on oatmeal agar and on ISP4 agar plates supplemented with nalidixic acid (75 μg/mL) and cycloheximide (50 μg/mL). A number of sporulating bacterial colonies were observed after one week of incubation at 28 °C and each colony was subsequently streaked on to a M_2-agar plate (glucose, 4.0 g/L; malt extract, 10.0 g/L; yeast extract, 4.0 g/L; and agar 15.0 g/L; pH of the medium was adjusted to 7.2 with 2 M NaOH prior to sterilization). Individual bacterial colonies were isolated from the second generation plate and fermented in 50 mL of soytone-glucose medium (glucose, 20 g/L; soytone, 10 g/L; $CaCO_3$, 2 g/L, and $CoCl_2$, 1 mg/L; pH 7.2) using 250 mL baffled Erlenmeyer flasks. Cultures were allowed to grow for 6 days at 28 °C with agitation (250 rpm). Amberlite XAD-16 (0.5 g, Sigma, St. Louis, MO, USA) resin was added to the culture 24 h prior to harvesting. Each individual culture was transferred to a 50 mL falcon tube and the mixture centrifuged at 3000 × *g* for 15 minutes. The supernatant was discarded and the mycelia-XAD resin portion was washed twice with 80 mL of distilled water prior to the addition of 15 mL methanol to generate the crude extract. The methanol extract was separated from the resin using Whatman filter paper (150 mm diameter, 11 μm pore size). Each extract was then subjected to HPLC/HR-ESI-MS analysis from which the degree of novelty for MS ions of major species was determined via comparison to the Natural Products Identifier AntiBase 2012 (Wiley corp., Hoboken, NJ). Based upon this analysis, *Streptomyces* sp. RM-7-15 was identified as among the strains capable of producing new metabolites.

Taxonomical Identification of *Streptomyces* sp. RM-7-15

Genomic DNA was isolated from a fully grown colony using InstaGene Matrix (Biorad, Hercules, CA, USA). DNA was purified using QIAquick PCR purification kit (Qiagen, Valencia, CA, USA). The partial 16S rRNA gene fragment was amplified using universal primers (27F, 5′-AGAGTTTGATCMTGGCTCAG-3′; 1492R, 5′-GGTTACCTTGTTACGACTT-3′) and Phusion High Fidelity DNA polymerase (New England Biolabs, Ipswich, MA, USA). QIAquick gel extraction kit (Qiagen) was used to gel-purify the amplified product to eliminate PCR inhibitors. The amplified fragment (1,242 bp) displayed 99% identity (BLAST search) to the 16S rRNA gene sequence of *Streptomyces yatensis* strain NBRC 101000. The sequence of 16S rRNA has been deposited in the NCBI nucleotide database with an accession number KC874988.

Fermentation, extraction, isolation and purification

Streptomyces sp. RM-7-15 was cultivated on M_2-agar (glucose, 10.0 g/L; malt extract, 10.0 g/L; yeast extract, 4.0 g/L; agar, 15.0 g/L) plates at 28 °C for 3 days. Chunks of agar with the fully-grown strain were used to inoculate four 250 mL Erlenmeyer baffled flasks, each containing 50 mL of medium A (soluble starch, 20.0 g/L; glucose, 10.0 g/L; peptone, 5.0 g/L; yeast extract, 5.0 g/L; NaCl, 4.0 g/L; K_2HPO_4, 0.5 g/L; $MgSO_4.7H_2O$, 0.5 g/L; $CaCO_3$, 2.0 g/L). Individual culture was grown at 28 °C with shaking (210 rpm) for 3 days and used as seed for the production scale fermentation. An aliquot of seed culture (3 mL) was used to inoculate 80–250 mL baffled flasks each containing 100 mL of A-medium. The fermentation was continued for 5 days at 28 °C with 200 rpm agitation. The obtained dark-green culture broth was centrifuged and filtered over Celite. The supernatant was extracted by mixing with XAD-16 (4%) resin overnight, followed by filtration. The resin was washed with water (3 × 800 mL) followed by extraction with MeOH (3 × 1200 mL). The methanol extract was subsequently evaporated *in vacuo* at 38 °C to afford 14.32 g of dark-green oily crude extract. The biomass (mycelium) was extracted with MeOH (3 × 800 mL) followed by acetone (1 × 500 mL) and then the recovered organics were evaporated *in vacuo* at 38 °C to yield 65.4 g of brown oily crude extract. Since the targeted metabolites were mainly predominate in the XAD-extract, this extract was advanced to the following work up and isolation procedure.

Fractionation of the XAD-16 extract (14.32 g) by silica gel column chromatography (column 5 × 60 cm, 300 g) with a gradient of 0–100% MeOH-CH_2Cl_2, resulted in the generation of following fractions: 1.0 L 0% MeOH → fraction FI (75.0 mg); 1.0 L 3% MeOH → fraction FII (0.36 g); 1.0 L 5% MeOH → fraction FIII (0.42 g); 1.0 L 7% MeOH → fraction FIV (1.054 g); 1.0 L 10% MeOH → fraction FV (0.71 g); 0.5 L 15% MeOH → fraction FVI (0.43 g); 0.5 L 20% MeOH → fraction FVII (0.23 g); 0.5 L 40% MeOH → fraction FVIII (0.38 g); 0.5 L 80% MeOH → fraction FIX (2.86 g); and 0.8 L 100% MeOH → fraction FX (2.56 g). Based upon TLC analysis, fraction I was determined to contain mostly fats. Further purification of fraction II using Sephadex LH-20 (CH_2Cl_2/40% MeOH, 2.5 × 50 cm) followed by separation via silica gel chromatography (CH_2Cl_2/3% MeOH, 3.5 × 30 cm) and HPLC afforded herbimycin A (yellow solid, 190.3 mg). Fractions FIII and FIV were combined based on the similarities of HPLC and TLC profiles to afford 1.45 g total amount. Sequential purification using Sephadex LH-20 (CH_2Cl_2/40% MeOH, 2.5 × 50 cm), silica gel column (CH_2Cl_2/3% MeOH, 3.5 × 30 cm) and then HPLC yielded dihydro-herbimycin A (white powder, 283.7 mg) along with herbimycin A (yellow solid, 60.5 mg). Isolated dihydro-herbimycin A was unstable and rapidly oxidized to herbimycin A within 10 minutes. This spontaneous oxidation was confirmed through the comparative analyses of UV and LC-MS profiles of the freshly isolated dihydro-herbimycin A and the standard herbimycin A. Purification of fraction FV (0.71 g) using PTLC (CH_2Cl_2/5% MeOH, 20 × 20 cm, 4 plates), followed by Sephadex LH-20, afforded herbimycin A (yellow solid, 55.0 mg), dihydro-herbimycin A (white powder, 43.1 mg) and the new ansamycin analogue herbimycin D (**1**; pale-yellow solid, 38.9 mg). Based on HPLC and TLC profiles, fractions FVI to FVIII were combined (1.04 g dry wt.), and subjected to sequential purification using Sephadex LH-20, preparative TLC and then semi-preparative HPLC to yield bicyclomycin (colorless solid, 35.5 mg, see supporting information) along with the new *ortho*-quinone ansamycin analogue herbimycin E (**2**; purble solid, 16.9 mg). Preliminary analyses indicated sugars as the major constituents of the fractions FIX and FX.

In the same manner, fractionation of the mycelial extract (65.4 g) by silica gel column chromatography (column 7.5 × 80 cm, 600 g) with a gradient of 0–100% MeOH-CH_2Cl_2, resulted in the generation of ten fractions (FI-FXI). Purification of sub-fraction FIV (0.23 g) using semi-preparative HPLC (MeCN-H_2O gradient) afforded herbimycin F (**3**; white solid, 2.20 mg). The remaining fractions and sub-fractions obtained from the mycelium extract lacked herbimycin analogues based on HPLC and TLC analyses (See supporting information, Figure S2).

Herbimycin D (1)—$C_{32}H_{45}N_3O_9S$ (647); pale-yellow solid; UV-absorbing (254 nm); dark-blue, turned to yellowish-green after few minutes then to reddish-brown following treatment with anisaldehyde/H_2SO_4 spray; R_f 0.44 (silica gel, 15% MeOH-CH_2Cl_2), 0.31 (silica gel, 7% MeOH-CH_2Cl_2); UV/vis (MeOH) λ_{max} (log ε) 246 (4.48), 320 sh (3.65) nm; ^{1}H NMR (CD_3OD, 400 MHz) and ^{13}C NMR (CD_3OD, 100 MHz), see Table 1; (−)-APCI-MS: *m/z* 646 $[M - H]^-$, 1293 $[2M - H]^-$; (+)-APCI-MS: *m/z* 648 $[M + H]^+$, 1295 $[2M + H]^+$; (+)-HR-ESI-MS: *m/z* 670.2768 $[M + Na]^+$ (calcd for $C_{32}H_{45}N_3O_9SNa$, 670.2769), and *m/z* 648.2946 $[M + H]^+$ (calcd for $C_{32}H_{46}N_3O_9S$, 648.2949); (−)-HR-ESI-MS: *m/z* 646.2849 $[M - H]^-$(calcd 646.2804 for $C_{32}H_{44}N_3O_9S$).

Herbimycin E (2)—$C_{30}H_{42}N_2O_{10}$ (590); purple solid; UV-absorbing (254 nm), blue-violet coloration with 2 N NaOH; dark-blue with anisaldehyde/H_2SO_4 spray; R_f 0.26 (silica gel, 8% MeOH-CH_2Cl_2), 0.41 (silica gel, 10% MeOH-CH_2Cl_2); UV/vis (MeOH) λ_{max} (log ε) 232 (4.54), 246 sh (4.52), 532 sh (3.20) nm; ^{1}H NMR (CD_3OD, 400 MHz) and ^{13}C NMR (CD_3OD, 100 MHz), see Table 1; (−)-APCI-MS: *m/z* 589 $[M - H]^-$, 1179 $[2M - H]^-$; (+)-APCI-MS: *m/z* 591 $[M + H]^+$, 608 $[M + NH_4]^+$, 613 $[M + Na]^+$, 1198 $[2M + NH_4]^+$; (+)-

HR-ESI-MS: *m/z* 613.2740 $[M + Na]^+$ (calcd for $C_{30}H_{42}N_2O_{10}Na$, 613.2732), *m/z* 608.3187 $[M + NH_4]^+$ (calcd for $C_{30}H_{46}N_3O_{10}$, 608.3178), and *m/z* 591.2917 $[M + H]^+$ (calcd for for $C_{30}H_{43}N_2O_{10}$, 591.2912); (−)-HR-ESI-MS: *m/z* 589.2795 $[M - H]^-$ (calcd 589.2767 for $C_{30}H_{41}N_2O_{10}$).

Herbimycin F (3)—$C_{28}H_{40}N_2O_9$ (548); white solid; UV non-absorbing (254 nm); reddish-brown with anisaldehyde/H_2SO_4 spraying agaent; R_f 0.21 (silica gel, 10% MeOH-CH_2Cl_2); UV/vis (MeOH) λ_{max} (log ε) 204 (4.12), 218 (4.07), 299 (3.25) nm; ^{1}H NMR (CD_3OD, 500 MHz) and ^{13}C NMR (CD_3OD, 100 MHz), see Table 1; (+)-APCI-MS: *m/z* 566 $[M + NH_4]^+$; (−)-APCI-MS: *m/z* 547 $[M - H]^-$, 1095 $[2M - H]^-$; (+)-ESI-MS: *m/z* 571 $[M + Na]^+$; (−)-ESI-MS: *m/z* 547 $[M - H]^-$; (+)-HR-ESI-MS: *m/z* 566.3075 $[M + NH_4]^+$ (calcd for $C_{28}H_{44}N_3O_9$, 566.3072), *m/z* 571.2629 $[M + Na]^+$ (calcd for $C_{28}H_{40}N_2O_9Na$, 571.2626), and *m/z* 1119.5401 $[2M + Na]^+$ (calcd for $C_{56}H_{80}N_4O_{18}Na$, 1119.5360); (−)-HR-ESI-MS: *m/z* 547.2838 $[M - H]^-$ (calcd 547.2661 for $C_{28}H_{39}N_2O_9$) and *m/z* 1095.5757 $[2M - H]^-$ (calcd 1095.5394 for $C_{56}H_{79}N_4O_{18}$).

Cell Viability Assay

A resazurin-based cytotoxicity assay, also known as the AlamarBlue assay, was used to assess the cytotoxicity of agents against the human lung non-small cell carcinoma cell line A549 cell line where cell viability was measured via reduction of resazurin (7-hydroxy-10-oxido-phenoxazin-10-ium-3-one) to its fluorescent product resorufin. A549 (ATCC, Manassas, VA, USA) was grown in DMEM/F-12 Kaighn's modification and MEM/EBSS media, respectively (Thermoscientific, Rockford, IL, USA) with 10% heat-inactivated fetal bovine serum (FBS), 100 μg/mL penicillin, 100 mg/mL streptomycin, and 2 mM L-glutamine. Cells were seeded at a density of 2×10^3 cells per well onto 96-well culture plates with clear bottom (Corning, NY, USA), incubated 24 h at 37 °C in a humidified atmosphere containing 5% CO_2 and were exposed to known toxic (1.5 mM hydrogen peroxide, 10 mg/mL actinomycin D) or test compounds for 2 days. Resazurin (150 mM, Sigma, St. Louis, MO, USA) was added to each well, the plate was shaken gently for 10 seconds and incubated for another 3 h (A549 cells) in 37 °C incubator to allow viable cells to convert resazurin into resorufin. The fluorescence intensity for resorufin was detected on a scanning microplate spectrofluorometer FLUOstar Omega (BMG Labtech, Cary, NC, USA) using an excitation wavelength of 560 nm and an emission wavelength of 590 nm. The assay was repeated in three independent replications. In each replication, the emission of fluorescence of resorufin values in treated cells were normalized to, and expressed as, a percent of the mean resorufin emission values of positive control (untreated, metabolically active cells; 100%, all cells are viable).

Hsp90α competition binding assay

The commercial Hsp90 assay kit (BPS Bioscience, San Diego, CA) was used compare the relative affinities of standards (geldanamycin and herbimycin A) to newly discovered herbimycin analogues following the manufacturer's protocol. This assay is based upon the use of a fluorescein-5-isothiocyanate linked geldanamycin (FITC-GM) and purified recombinant Hsp90α in a fluorescence polarization-based competition assessment that has been used for the identification and/or comparison of Hsp90α inhibitors.[34] Represenative assays contained 100 nM FITC-GM, 700 ng Hsp90α (lot#100125, BPS Bioscience) and 0–100 nM inhibitor in 20 mM HEPES pH 7.3 containing 50 mM KCl, 5 mM $MgCl_2$, 20 mM Na_2MoO_4, 0.01% Triton X-100, 100 μg/mL bovine serum albumin and 2 mM DTT. Assay mixtures were incubated for 3 hours in black 96-well low binding NUNC microplates at room temperature and the change in fluorescence polarization (λ_{ex}=485 nm; λ_{em}=530 nm) was measured using a PerkinElmer Victor3 (Waltham, MA) with a 505 nm beam splitter. All polarization values were expressed in millipolarization units (mP) that were calculated

using the equation $\mathrm{mP}=1000\mathrm{x}\ [(I_S-I_{SB})-(I_P-I_{PB})]/[(I_S-I_{SB})+(I_P-I_{PB})]$, where I_S is the parallel emission intensity, I_P is the perpendicular emission intensity, and I_{SB} and I_{PB} are the corresponding measurements for background (buffer). FITC-GM binds tightly to Hsp90α (K_d of 11.83 nM for lot#100125, BPS Bioscience) and this comparative study was based upon the recorded polarization with a particular inhibitor minus polarization of free FITC-GM (without Hsp90α in the well) as previously described.[34] For each assay, background wells (buffer only), tracer controls (free, FITC-GM only), and bound GM controls (FITC-GM in presence of Hsp90α) were included on the plate. The fraction of tracer bound to Hsp90 was correlated to the mP values and plotted against values of competitor concentration. A preliminary dose range study revealed 33 nM as an optimal concentration for the competitive binding assay and therefore, subsequent binding assays were carried out at 33 nM concentration in triplicate. Positive controls for this study included unlabeled geldanamycin and herbimycin A.

Antimicrobial Activity Assays

A fungus strain *Saccharomyces cerevisiae* (ATCC 204508), and two bacterial strains *Staphylococcus aureus* (ATCC 6538) and *Salmonella enterica* (10708) were used as model strains for antimicrobial susceptibility assays. *S. cerevisiae*, *S. enterica* and *S. aureus* were grown in liquid or on agar plates using YAPD (ATCC medium number 1069), nutrient broth (BD 234000) and tryptic soy broth (BD211825), respectively. Individual strains were grown in 5 mL medium for 16 h at 37 °C with shaking (200 rpm). An aliquot of a fully grown culture (100 μL) was diluted to 30 mL using sterile liquid medium. Aliquots (160 μL) of each diluted culture were then transferred into the individual well of a 96 well plate supplied with 2 μL of herbimycins D-F (**1–3**) and A (**4**). Various concentrations of compounds **1–4** (range 1–125 μM final concentration) were maintained to assess the antimicrobial activities and compared to the negative control containing vehicle (DMSO) alone and positive controls (200 μg ampicillin and kanamycin for *S. enterica* and *S. aureus*; 50 μg cycloheximide for *S. cerevisiae*). The culture plate was incubated at 37 °C for 16 h with shaking (200 rpm) and then the OD_{600} of each well measured using a scanning microplate spectrofluorometer FLUOstar Omega (BMG Labtech, Cary, NC, USA). The acquired OD_{600} values were normalized to the negative control wells (100% viability).

Supplementary Material

Refer to Web version on PubMed Central for supplementary material.

Acknowledgments

This work was supported in part by the University of Kentucky, College of Pharmacy; the University of Kentucky, Markey Cancer Center; and the National Center for Advancing Translational Sciences (UL1TR000117).

References and Notes

1. Floss HG. J Nat Prod. 2006; 69:158–169. [PubMed: 16441092]
2. Floss HG. Nat Prod Rep. 1997; 14:433–452. [PubMed: 9364776]
3. Kibby JJ, Mcdonald IA, Rickards RW. J Chem Soc-Chem Commun. 1980:768–769.
4. Kim CG, Yu TW, Fryhle CB, Handa S, Floss HG. J Biol Chem. 1998; 273:6030–6040. [PubMed: 9497318]
5. Floss HG, Yu TW. Chemical reviews. 2005; 105:621–632. [PubMed: 15700959]
6. August PR, Tang L, Yoon YJ, Ning S, Muller R, Yu TW, Taylor M, Hoffmann D, Kim CG, Zhang X, Hutchinson CR, Floss HG. Chem Biol. 1998; 5:69–79. [PubMed: 9512878]
7. Campbell EA, Korzheva N, Mustaev A, Murakami K, Nair S, Goldfarb A, Darst SA. Cell. 2001; 104:901–912. [PubMed: 11290327]

8. Stebbins CE, Russo AA, Schneider C, Rosen N, Hartl FU, Pavletich NP. Cell. 1997; 89:239–250. [PubMed: 9108479]
9. Tomioka H. Curr Pharm Des. 2006; 12:4047–4070. [PubMed: 17100611]
10. Ramos-e-Silva M, Rebello PF. Am J Clin Dermatol. 2001; 2:203–211. [PubMed: 11705247]
11. Sepkowitz KA, Raffalli J, Riley L, Kiehn TE, Armstrong D. Clin Microbiol Rev. 1995; 8:180–199. [PubMed: 7621399]
12. Lalloo UG, Ambaram A. Curr HIV/AIDS Rep. 2010; 7:143–151. [PubMed: 20559756]
13. Centers for Disease Control and Prevention. Recommendations for use of an isoniazid-rifapentine regimen with direct observation to treat latent Mycobacterium tuberculosis infection. MMWR Morb Mortal Wkly Rep. 2011:1650–1653. [PubMed: 22157884]
14. Li T, Ni S, Jia C, Wang H, Sun G, Wu L, Gan M, Shan G, He W, Lin L, Zhou H, Wang Y. J Nat Prod. 2012; 75:1480–1484. [PubMed: 22849774]
15. Wu CZ, Jang JH, Woo M, Ahn JS, Kim JS, Hong YS. Appl Environ Microbiol. 2012; 78:7680–7686. [PubMed: 22923401]
16. Jeso V, Cherry L, Macklin TK, Pan SC, LoGrasso PV, Micalizio GC. Org Lett. 2011; 13:5108–5111. [PubMed: 21866939]
17. Yang YH, Fu XL, Li LQ, Zeng Y, Li CY, He YN, Zhao PJ. J Nat Prod. 2012; 75:1409–1413. [PubMed: 22742732]
18. Jhaveri K, Taldone T, Modi S, Chiosis G. Biochim Biophys Acta. 2012; 1823:742–755. [PubMed: 22062686]
19. Biamonte MA, Van de Water R, Arndt JW, Scannevin RH, Perret D, Lee WC. J Med Chem. 2010; 53:3–17. [PubMed: 20055425]
20. Funayama S, Anraku Y, Mita A, Yang ZB, Shibata K, Komiyama K, Umezawa I, Omura S. J Antibiot. 1988; 41:1223–1230. [PubMed: 3182402]
21. Mochizuki J, Kobayashi E, Furihata K, Kawaguchi A, Seto H, Otake N. J Antibiot. 1986; 39:157–161. [PubMed: 3512505]
22. Grunicke H, Pushendrof B, Werchau H. Rev Physiol Biochem Pharmacol. 1976; 75:69–96. [PubMed: 59940]
23. Kasik JE, Monick M, Thompson JS. Antimicrob Agents Chemother. 1976; 9:470–473. [PubMed: 4011]
24. Bernardo J, Ossola RJ, Spotila J, Crandall KA. Biol Lett. 2007; 3:695–698. [PubMed: 17711816]
25. Stein, BA.; Kutner, LS.; Adams, JS. Precious Heritage: The Status of Biodiversity in the United States. Oxford University Press; Oxford, UK: 2000.
26. O'Keefe JMK, Henke KR, Hower JC, Engle MA, Stracher GB, Stucker JD, Drew JW, Staggs WD, Murray TM, Hammond ML, Adkins KD, Mullins BJ, Lemley EW. Sci Total Environ. 2010; 408:1628–1633. [PubMed: 20071005]
27. Hower JC, Henke K, O'Keefe JMK, Engle MA, Blake DR, Stracher GB. Int J Coal Geol. 2009; 80:63–67.
28. Laatsch, H. The natural compound identifier. Wiley-Vch; 2012. AntiBase.
29. Lin L, Ni S, Wu L, Wang Y, Wang Y, Tao P, He W, Wang X. Biosci Biotechnol Biochem. 2011; 75:2042–2045. [PubMed: 21979086]
30. Hosokawa N, Naganawa H, Hamada M, Iinuma H, Takeuchi T, Tsuchiya KS, Hori M. J Antibiot. 2000; 53:886–894. [PubMed: 11099221]
31. Cricchio R, Antonini P, Sartori G. J Antibiot. 1980; 33:842–846. [PubMed: 7429988]
32. Ni SY, Wu LZ, Wang HY, Gan ML, Wang YC, He WQ, Wang YG. J Microbiol Biotechnol. 2011; 21:599–603. [PubMed: 21715966]
33. Schlegel B, Hanel F, Gollmick FA, Saluz HP, Grafe U. J Antibiot. 2003; 56:917–922. [PubMed: 14763557]
34. Hu Z, Liu Y, Tian ZQ, Ma W, Starks CM, Regentin R, Licari P, Myles DC, Hutchinson CR. J Antibiot. 2004; 57:421–8. [PubMed: 15376554]

35. Lundgren K, Zhang H, Brekken J, Huser N, Powell RE, Timple N, Busch DJ, Neely L, Sensintaffar JL, Yang YC, McKenzie A, Friedman J, Scannevin R, Kamal A, Hong K, Kasibhatla SR, Boehm MF, Burrows FJ. Mol Cancer Ther. 2009; 8:921–929. [PubMed: 19372565]

36. Zhao H, Michaelis ML, Blagg BS. Adv Pharmacol. 2012; 64:1–25. [PubMed: 22840743]

37. Abdelfattah MS, Kharel MK, Hitron JA, Baig I, Rohr J. J Nat Prod. 2008; 71:1569–1573. [PubMed: 18666798]

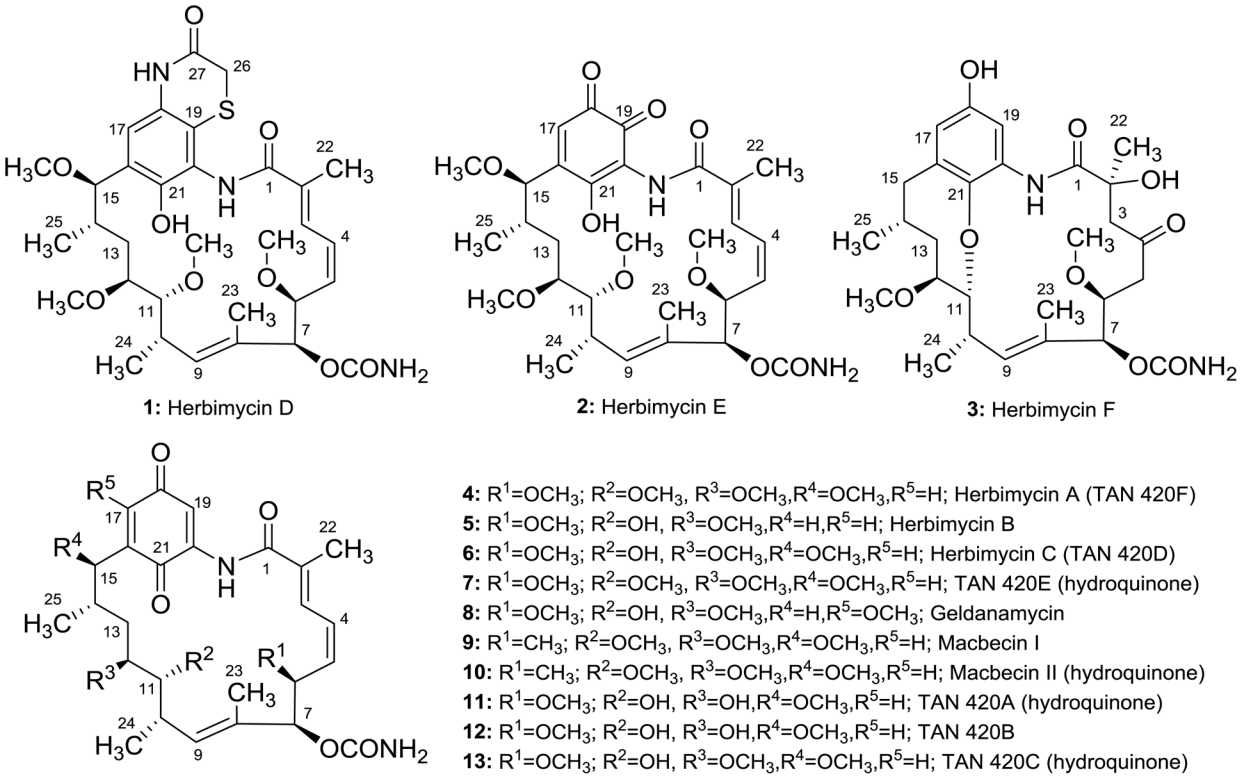

Figure 1.
Structure of the new herbimycins D-F (**1–3**) along with the related analouges **4–13**

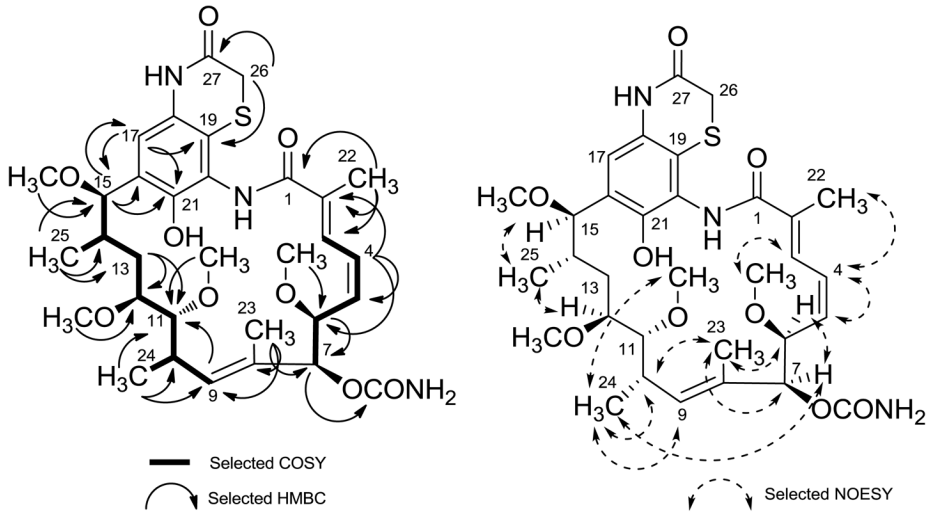

Figure 2.
Selected ^{1}H ^{1}H COSY (▬), HMBC (→) and NOESY (⋯) correlations in Herbimycins D (**1**)

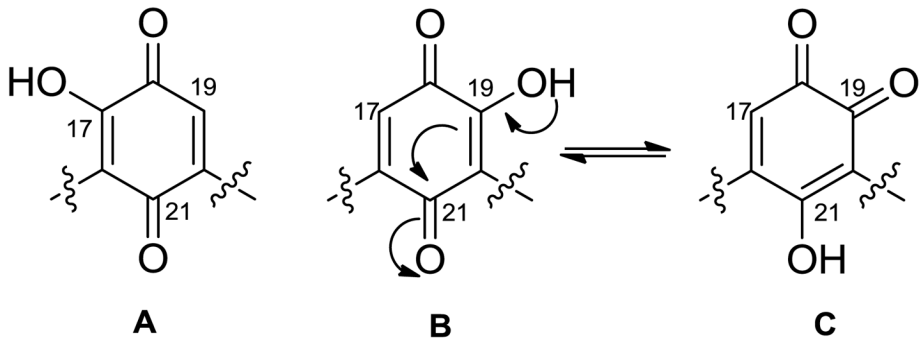

Figure 3.
Structural possibilities for the aromatic ring in compound **2**.

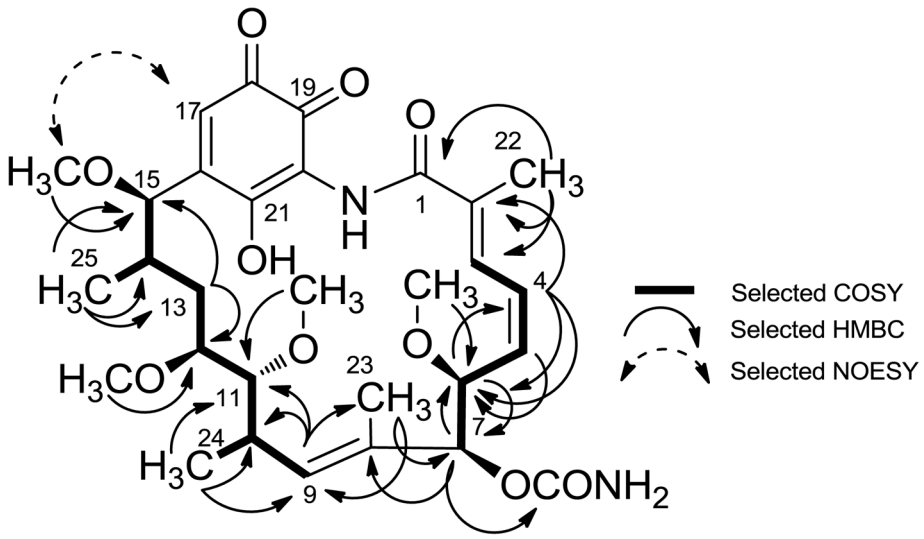

Figure 4.
Selected ^{1}H ^{1}H COSY (▬), HMBC (→) and NOESY (⋯) correlations in Herbimycins E (**2**)

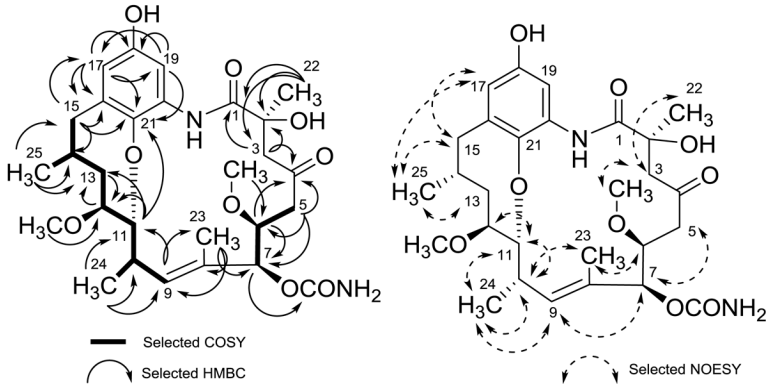

Figure 5.
Selected ^{1}H ^{1}H COSY (▬), HMBC (→) and NOESY (⋯) correlations in Herbimycin F (**3**)

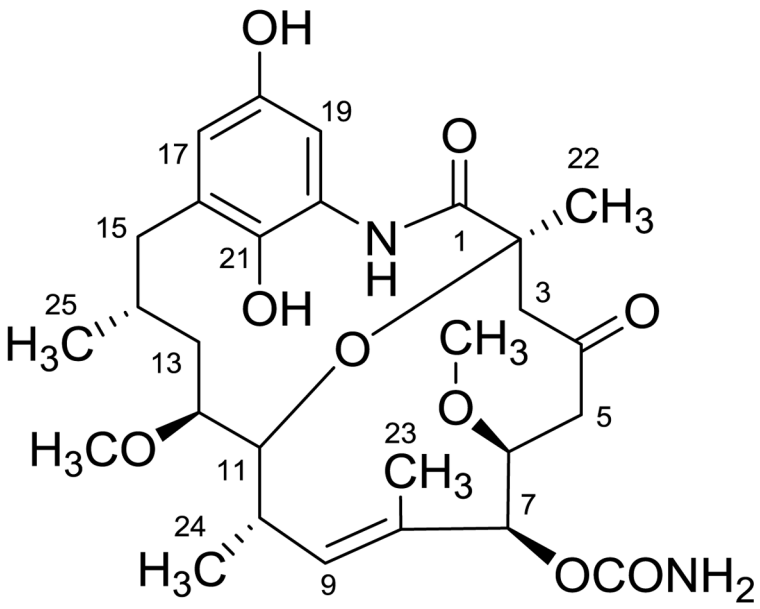

Figure 6.
Structure possiblity **14**, containing the ether linkage between C-2 and C-11

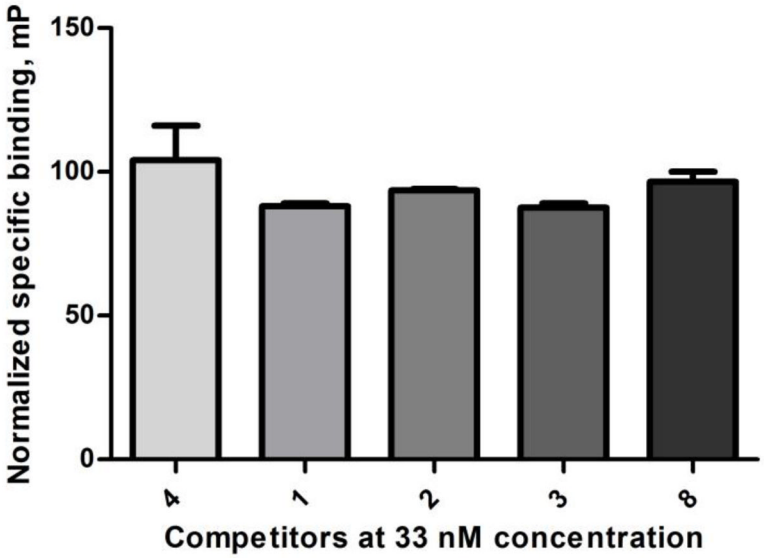

Figure 7.
Comparision of binding affinity of compounds **1–4** and geldanamycin (**8**) with Hsp90α

Table 1

^{13}C and ^{1}H NMR data of herbimycins D–F (**1–3**) in CD_3OD (mult., *J* in [Hz])

Position	Herbimycin D (1) [a]		Herbimycin E (2) [a]		Herbimycin F (3)[a]	
	δ_C (100 MHz)	δ_H (400 MHz)	δ_C (100 MHz)	δ_H (400 MHz)	δ_C (100 MHz)	δ_H (500 MHz)
1	177.1, C	-	177.8, C	-	177.5, C	-
2	136.5, C	-	137.4, C	-	80.1, C	-
3	124.3, CH	6.02, brm	124.2, CH	6.49, brm	50.2, CH_2	3.42, d (16.5) 2.98, d (16.0)
4	130.3, CH	6.37, t (11.6)	130.8, CH	6.36, t (11.2)	205.8, C	-
5	129.9, CH	5.12, brm	129.5, CH	5.10, t (10.0)	49.9, CH_2	2.82, dd (19.0, 8.5) 2.55, dd (19.0, 2.0)
6	76.9, CH	3.87, brm	76.7, CH	4.20, brm	76.2, CH	3.97, ddd (9.5, 9.0, 3.0)
6-OCH_3	56.7, CH_3	3.08, s	56.5, CH_3	3.09, s	60.5, CH_3	3.44, s
7	82.4, CH	4.87, brs	83.4, CH	4.81, brm	85.3, CH	4.92, d (9.5)
7-O$\underline{CO}NH_2$	159.3, C	-	159.4, C	-	159.2, C	-
8	131.3, C	-	131.4, C	-	132.0, C	-
9	135.3, CH	5.20, d (10.4)	136.0, CH	5.19, d (10.4)	137.2, CH	5.39, brd (10.5)
10	36.5, CH	2.38, brm	37.0, CH	2.23, brm	36.4, CH	2.50, m
11	85.3, CH	3.25, m	84.7, CH	3.28, m	75.1, CH	3.60, brdd (8.5, 1.5)
11-OCH_3	61.8, CH_3	3.52, s	61.8, CH_3	3.48, s	-	-
12	82.7, CH	3.00, m	81.4, CH	4.53, m	86.8, CH	3.19, brd (6.0)
12-OCH_3	57.3, CH_3	3.35, s	57.5, CH_3	3.18, s	57.1, CH_3	3.46, s
13	27.1, CH_2	1.74-1.60, m	26.8, CH_2	1.74-1.60, m	37.9, CH_2	1.54, m 1.42, m
14	36.5, CH	2.26, m	34.8, CH	2.23, brm	35.5, CH	1.46, m
15	82.7, CH	4.69, brm	82.3, CH	3.00, brd (8.8)	38.7, CH_2	3.33, dd (11.0, 3.0)*, 1.66, t (11.0)
15-OCH_3	57.2, CH_3	3.22, s	57.2, CH_3	3.32, s	-	-
16	128.5, C	-	151.5, C	-	123.4, C	-
17	116.1, CH	6.73, s	129.9, CH	6.24, s	113.9, CH	6.21, d (3.0)
18	126.9, C	-	190.1, C	-	153.0, C	-
19	117.6, C	-	181.7, C	-	101.8, CH	6.24, d (2.5)

Position	Herbimycin D (1) [a]		Herbimycin E (2) [a]		Herbimycin F (3)[a]	
	δ_C (100 MHz)	δ_H (400 MHz)	δ_C (100 MHz)	δ_H (400 MHz)	δ_C (100 MHz)	δ_H (500 MHz)
20	131.8, C	-	119.9, C	-	128.4, C	-
21	148.1, C	-	163.8, C	-	153.0, C	-
22	14.3, CH_3	2.01, s	14.1, CH_3	1.92, s	23.1, CH_3	1.31, s
23	13.0, CH_3	1.23, brs	13.1, CH_3	1.32, brs	11.9, CH_3	1.52, s
24	18.9, CH_3	0.98, d (6.4)	19.0, CH_3	0.95, brd (5.6)	17.7, CH_3	1.06, d (6.5)
25	15.6, CH_3	0.69, brd (5.2)	17.1, CH_3	0.59, brd (5.6)	21.4, CH_3	0.76, d (6.0)
26	30.0, CH_2	3.62, d (14.8), 3.31, d (14.8)	-	-	-	-
27	166.8, C	-	-	-	-	-

[a] See also supporting information for NMR spectra.

* Overlapped with the solvent peak